International Journal of Imaging,
Autumn 2010, Volume 4, Number A10,
Int. J. Imag.; ISSN 0974-0627;


# Integration of Colour and Texture Distributions for Skin Cancer Image Segmentation

**Padmapriya Nammalwar, Ovidiu Ghita,** and **Paul F. Whelan**

Vision Systems Group, School of Electronic Engineering,
Dublin City University, Dublin 9, Ireland
nammalp2@mail.dcu.ie, ghitao@eeng.dcu.ie, paul.whelan@eeng.dcu.ie

**ABSTRACT**

*This study presents an efficient way to segment the skin cancer images. A novel method is proposed that combines colour and texture for the segmentation of skin lesions from unaffected skin region in an image. The distributions of colour and texture features provide a platform for the discrimination of skin lesions. The segmentation results are evaluated quantitatively by means of a comparative experiment on a set of skin cancer images. The evaluation of the proposed method is based on the comparison with Live Wire segmentation technique. The results indicate that the proposed methodology proved effective and efficient for the skin cancer image segmentation.*

**Keywords:** Colour, Melanoma, Segmentation, Skin cancer, Texture.

**Mathematics Subject Classification Numbers:** 68U10

## I. INTRODUCTION

Skin cancer is the most prevalent form of human cancer which is a malignant tumor on the skin. Over exposure to the sun is one cause for skin cancer. There are different types of skin cancer and some are likely to be fatal. Skin cancers can be classified into melanoma and non-melanoma. Melanoma is a malignancy of the cells which give the skin its colour (melanocytes). The two most frequent types of non-melanoma skin cancer are Basal Cell Carcinomas and Squamous Cell Carcinoma. In addition, there are a number of other less common skin cancers including Merkel cell tumors, cutaneous lymphomas, and sarcomas [1]. Melanoma is the most dangerous form of skin cancer. It can spread through the whole body and is usually fatal. If detected early, the cure rate for melanoma is almost 100 percent. Late detection, when the melanoma is more than three millimeters deep, results in only a 59 percent survival rate. Melanoma's are much less common than non-melanoma's, but they account for most of the mortality from skin cancers. Detection of malignant melanoma in its early stages considerably reduces morbidity and mortality [2]. Early detection also saves hundreds of millions of money that is spent on the advanced disease. People are considered more at risk if they have lots of moles, are fair skinned with blue eyes, tend to sunburn easily or have freckles [3]. The rate of melanoma cases worldwide is increasing faster than any other cancer, with an annualized rate of increase of six percent. While in the thirties of the century one out of hundred thousand people living in the United States or Europe suffered from melanoma. This number has risen to fifteen out of hundred thousand nowadays with the tendency still increasing [4]. Clinical features of pigmented lesions suggestive of skin cancer are known as the ABCD's of the skin cancer:

- Asymmetry;
- Border irregularity;
- Colour variation;
- Diameter greater than 6 mm.

There are various image analysis techniques developed to measure these features. During the last years, a significant improvement in early tumor recognition has been achieved by using the epiluminescence microscopy (ELM). This technique uses oil immersion to render the epidermis translucent thus giving insight into subsurface structures of the skin which are not visible otherwise.

This delivers a set of new features which have turned out to improve the reliability of early diagnosis considerably. The ELM criteria used by dermatologist for the classification of pigmented skin lesions are briefly outlined as follows [5]:

- Pigmentation - Asymmetry of pigmentation is indicative of malignant lesion.
- De-pigmentation - Represents absence or diminution of pigment within a pigmented lesion. In benign lesions, de-pigmentation is regular and usually found at the center, whereas in malignant lesions it is irregular located anywhere in the lesion, and found at the periphery.
- Colour - Irregular bluish or grey-blue areas can almost exclusively be found in malignant lesions.
- Brown Globules in benign lesions - They are uniform in size and shape and regularly distributed, whereas variations in size and shape and irregular distribution indicate malignity.
- Black Dots - When present in benign lesions, they only occur at the center and are regular in size, shape and distribution. In malignant lesions they also occur at the periphery, vary in size and shape, and are irregularly distributed.

Measurement of image features for diagnosis of the skin cancer requires the detection of lesions and localization in an image. It is essential to determine the lesion boundaries accurately so that measurements such as maximum diameter, irregularity of the boundary, and colour characteristics can be accurately computed. As a first step in skin cancer identification, the lesion boundaries are delineated by various image segmentation techniques. In this research work, colour and texture information from an image is used in a novel framework for segmentation. Different frameworks have been developed by researchers for colour texture segmentation and most of the frameworks were designed for a specific application. The framework developed in this work combines the distributions of colour and the distributions of texture to discriminate the colour textured regions. The framework can be applied to various scientific fields and one such application is skin cancer identification [6]. Various factors affect the segmentation of skin cancer images and they are as follows:

- The skin lesions have complex structure, large variations in size as well as complex colours in the skin.
- The lesion is contrast to the surrounding skin.
- The borders of lesions are not always well defined.
- The influence of small structures, hairs, bubbles, light reflection, and other artifacts.
- The influence of the skin lesions in the surrounding regions.

These factors make the segmentation more complex. To analyze skin lesions, it is necessary to accurately locate and isolate the lesions. The description of the border aspect appears to be an important feature for clinical judgment [7]. Some border descriptors, such as border irregularity and the presence of abrupt border cutters have been considered as predictors of malignancy. Also, the variation in colour signifies the malignancy of the lesion. Hence effective discrimination of the skin lesions is based on the distribution of texture and colour features in this study.

This study uses Local Binary Pattern (LBP) [8] as the texture feature extraction technique. Colour features were derived based on *k*-means algorithm which clusters the input image by organizing the data into *k* different clusters. The distributions of LBP and the distributions of colour clustered labels

were combined for colour texture segmentation. This unification of colour and texture increases the efficiency of colour texture segmentation. The distributions of the texture and the distributions of the colour discriminates the colour textured image. The segmentation helps to diagnose the skin lesions in the early stages. A pre-processing step is adopted to remove the influence of skin lesions in the surrounding regions and also the influence of small structures, hairs, bubbles etc. The skin cancer images obtained from references [3] are in graphics interchange format (.GIF). They were converted to bitmap format to apply the segmentation procedure. Eighteen skin cancer images are considered for the application database.

## II. FRAMEWORK FOR COLOUR TEXTURE IMAGE SEGMENTATION

A novel way of combining texture and colour information's for the colour texture segmentation was developed that makes the segmentation robust and efficient for different types of images. The steps followed in this method are outlined below:
Initially the features were extracted using feature extraction techniques, in which image information is reduced to a small set of descriptive features.

- The LBP/C features are extracted from the average of the three planes in RGB colour space.
- The distribution of the texture features are used for texture discrimination.
- A Modified-Kolmogorov Smirnov (MKS) non-parametric statistical test is used as a similarity measure to discriminate the texture distributions.
- A hierarchical splitting method is used to split the image based on the texture descriptions using the similarity measure.
- An adaptive smoothing is performed to preserve the features and to obtain a good segmentation along the boundaries. This technique used as a preprocessing to remove noise and prevent over segmentation.
- An unsupervised k-means clustering algorithm is performed on the image to obtain the distribution of the colour clustered labels.
- Distribution of the texture features and the distribution of the colour clustered labels are used to describe the texture and the colour respectively.
- The distributions of colour and texture were used to derive the merger importance value between two adjacent regions. The Merger Importance value (MI) was calculated using the MKS statistic. Weights are included automatically to both texture and colour features in the histogram and are computed using the histograms of the colour labels.
- An agglomerative merging procedure based on the merging criteria determines the similarity between two different regions using MKS statistic, producing the segmented image.
- The final step is to refine the boundaries of the image. A boundary refinement algorithm based on the colour histograms enhances the segmented result to obtain the final segmented image.

## III. DETAILS OF COLOUR TEXTURE SEGMENTATION

### Feature Distributions

#### *Texture feature distributions*

The LBP concept developed by Ojala et al. [9] attempts to decompose the texture into small texture units. A texture unit is represented in a $3\times3$ neighborhood represented by $V = \{V_0, V_1, V_2, ...., V_8\}$ which generates $2^8$ possible standard texture units. In this regard, the LBP texture unit

$TU = \{E_1, E_2, ..., E_8\}$ is simply obtained by applying a simple threshold operation using the following rule:

$$E_i = \begin{cases} 0 & V_i < V_0 \\ 1 & V_i \geq V_0 \end{cases} \quad (1)$$

where $V_0$ is the central pixel of the $3 \times 3$ mask. The LBP is determined as follows:

$$LBP = \sum_{i=1}^{8} E_i \times 2^{i-1} \quad (2)$$

As the LBP does not take into consideration the contrast of the texture which is a measure of local greyscale variation, often the LBP is used in conjunction with a contrast measure. Here, the contrast measure is the normalized difference between the grey level of the pixels with a LBP value of 1 and the pixels with a grey-level 0 contained in the texture unit.

The distribution of the LBP/C of the image represents the texture spectrum. The LBP/C distribution is a 2D histogram of size $256 \times b$, where b is the number of bins for contrast measure. As suggested by Ojala et al. [9] we have used 8 bins for contrast measure (our experiments confirmed that best segmentation has been achieved when 8 bins have been used to sample the contrast measure). This 2D histogram is used as a texture discriminating feature in our implementation.

***Colour feature distributions***

This study uses the unsupervised clustering technique based on the *k*-means algorithm to cluster the colour features. The *k*-means algorithm is the simplest and most popular among the iterative clustering algorithms. The k-means algorithm organizes the objects into an efficient representation that characterizes the population being sampled. The number of clusters is generally image dependent so the initial guess is 10 clusters, this number is sufficient to capture all the relevant clusters. The distribution of the colour clusters is used for colour description. Detailed explanation of the clustering data can be found in [10].

**Modified Kolmogorov Smirnov (MKS)**

A nonparametric test MKS statistic was used for comparing LBP/C with colour clustered labels. This tests the hypothesis that two empirical feature distributions have been generated from the same population. MKS has the desirable property that it is invariant to arbitrary monotonic feature transformations [11]. The MKS statistic is defined as the sum of the absolute value of the discrepancies between the normalized cumulative distributions.

$$D(s,m) = \sum_{i=0}^{n} \left| \frac{F_s(i)}{n_s} - \frac{F_m(i)}{n_m} \right| \quad (3)$$

where $F_s(i)$ and $F_m(i)$ represents the sample cumulative distribution functions; $n_s$ and $n_m$ represents the number of pixels in the sample regions. Since MKS is normalised, it is advantageous over other statistical measures such as: G-statistic and the Chi square statistic.

**Adaptive Smoothing**

Various smoothing techniques are widely considered for different purposes in computer vision. The nonlinear smoothing preserves important features and also removes noise. Adaptive smoothing is a nonlinear smoothing which adapts pixel intensities to the local attributes of an image on the basis of discontinuity measures. The feature preserving adaptive smoothing algorithm proposed by Chen [12] was adopted in this study, where the local and contextual discontinuity measures are jointly used. The advantage of this smoothing technique is that the parameters in the given adaptive smoothing

algorithm critically determine the smoothing process. The parameters preserve the edges and removes noise. This procedure is used to prevent over segmentation.

**Segmentation Method**

***Hierarchical splitting***

The segmentation method followed is based on a split and merge computational model [13]. The first step involves recursively splitting the image hierarchically into four sub-blocks using only the LBP/C data. In this regard, the similarity measure between the resulting four sub-blocks is evaluated using the MKS. The uniformity of the region is evaluated by a decision factor as follows:

$$R = \frac{MKS_{max}}{MKS_{min}} > X \tag{4}$$

where $MKS_{max}$ and $MKS_{min}$ are the highest and lowest MKS values resulting after calculating the pair-wise MKS values of the four sub-blocks and X is a split threshold value. The splitting process continues until the stopping rule is satisfied or the block size is smaller than a predefined value (for this implementation the minimum block size has been set to $16 \times 16$). During the splitting procedure for each block two distributions are computed, the LBP/C distribution and the distribution of labels contained in the clustered data. Note that the splitting decision evaluates only the LBP/C MKS values. The choice of X is based on the testing for different values of X. The selection of X should be small to allow more split, rather less number of splits. An error occurs when a block defined by uniform texture is split into four blocks. In that situation the merging procedure can easily compensate for the over split. On the other hand, if several textures are considered as uniform then the error recovery is not possible.

***Agglomerative merging***

The second step applies an agglomerative merging procedure on the image resulting after splitting in order to join the adjacent regions that have similar characteristics. This procedure calculates the merging importance (MI) between any adjacent regions in the split image and the adjacent regions with the smallest MI value are merged. The MI value between two adjacent regions is calculated as follows:

$$MI = w_1 \times MKS_1 + w_2 \times MKS_2 \tag{5}$$

where $w_1$ and $w_2$ represent the corresponding weights for LBP/C histogram and colour histogram respectively and the $MKS_1$ and $MKS_2$ are the MKS statistics for texture (LBP/C) and colour histograms in the two adjacent regions. These adjacent regions are also referred to as the sample and model regions. The weights are automatically detected using a uniformity factor defined as the maximum of the ratio between colour clustered histogram and number of pixels in the two regions under consideration, the sample and the model regions.

$$k_j = \max\left\{\frac{Clust_j[i]}{N_p}\right\} \tag{6}$$

where $k_j$ represents the uniformity factor for the sample and the model regions respectively. The numerator in equation (6) represents the colour clustered histogram for the region. The denominator $N_p$ represents the number of pixels in the corresponding regions. If the difference between $k_1$ and $k_2$ is less than 0.1, i.e., both the sample and the model weights are more or less the same, then

$$w_2 = (k_1 + k_2)/2 \tag{7}$$

and

$$w_1 = 1 - w_2 \quad (8)$$

This indicates that colour influences more than texture, hence colour statistic is given more importance. On the other hand, if the difference between *k*'s is high, both the texture and the colour are given equal weights. The automatic selection of colour and texture weights provided a good result with minimum segmentation error [13]. This method followed a simple stopping rule,

$$\mathrm{Min}(\mathrm{MI}) > Y \quad (9)$$

where Min(MI) represents the minimum merger importance value. If this is greater than a threshold value Y then the merging procedure is halted. The agglomerative merging procedure resulted in blocky segmented image.

***Boundary refinement***

A new boundary refinement algorithm is developed and used for the improvement at the boundaries between various regions. A pixel is regarded as a boundary point if it is on the boundary of at least two distinct regions, i.e., its region label is different from at least one of its four neighbors. For an examined point *P*, a discrete square with a dimension "*d*" around the pixel was placed and the colour histogram for this region was computed. The corresponding colour histograms for the different neighboring points were calculated. The homogeneity of the square region and the *i*th neighboring region, *i*=1,2,...*l*...*n* region was computed. The pixel is reclassified if the MI value between adjacent regions and the region around the pixel under consideration is lower than the merge threshold. This procedure is iterative and proceeds until no pixels are relabeled. Reassigning pixels this way improves the accuracy of the segmentation process.

## IV. LIVE WIRE SEGMENTATION

The evaluation of the proposed colour texture segmentation method is based on comparing the results with that of Live Wire [14], segmentation results. In image segmentation, there are often situations when automatic segmentation techniques fail or lead to a suboptimal solution. As a consequence, an expert has to correct results manually. For interactive segmentation, an effective strategy is to exploit the synergy between a human operator who is superior in object recognition and an algorithm which is better in exact object delineation. The interactive Live Wire [14], algorithm utilizes methods from graph theory for achieving these abilities. An image constitutes a directed graph where the pixel vertices are graph nodes and oriented pixel edges represent edges of the graph. Graph edges are weighted with costs which are derived from image gradient magnitude and direction information. The basic problem of finding a boundary segment is therefore converted to finding a minimum-cost path between start and end of the segment. To find this optimal path, dynamic programming is used. A detailed explanation of the Live Wire segmentation can be obtained from reference [15].

## V. RESULTS AND DISCUSSION

The proposed segmentation method was tested based on the experiments using skin cancer images. 18 different representative skin lesion images were used for testing. The images consist of different skin lesions such as malignant melanoma, basal cell carcinoma and squamous cell carcinoma. The skin cancer images used were of varying size. It is observable that the lesions have large variations in size as well as in colour and contrast to the surrounding skin. In some skin cancer images, hairs surrounding the skin lesion can be observed, which would have disturbing influence on the deviation of the correct boundaries.

The significance and the necessity for the boundary refinement are shown in Fig 1 and Fig 2. Fig 3 and Fig 4 shows results after merging and boundary refinement. Agglomerative merging resulted in a

blocky segmented image. Boundary refinement enhances the blockiness and results in a smooth boundary. The proposed segmentation method was able to identify the lesion, the normal skin with different texture and coloured regions.

**Fig 1-4 (a) Results after agglomerative merging stage (b) Results after boundary refinement stage**

Fig 5.b and Fig 6.b shows lots of disturbance in the boundary refinement. This is due to the disturbance of hairs present in the skin. Also, the smoothing was not applied to show the influence of the disturbance from various factors. On applying the smoothing this resulted in a good segmentation. Again, Figs 5 and 6 shows the influence of hairs, texture and colour of the skin. Figures 5.c and 6.c are enlarged to show the boundary clearly. The inclusion of adaptive smoothing enhances the result and avoids the distortion.

**Fig 5-6. (a) Result after agglomerative merging stage (b) Result after boundary refinement without preprocessing (c) Result after boundary refinement with preprocessing**

Colour is one of the significant features in the examination of skin lesion. Typical examples of lesions show reddish, bluish, grey and black areas and spots. The fine variation in the colour is identified and segmented accurately. The distribution of texture and colour features presents significant information; hence the segmentation based on the two features is appropriate. This allows the isolation of lesion from healthy skin and extracts homogeneous coloured regions separately. The boundary, indicated by yellow line, obtained with Live Wire segmentation is shown in Fig 7.a. The boundary obtained with colour texture segmentation, indicated by white line, is shown in Fig 7.b. The colour texture segmentation resulted in two boundaries based on the colour gradient present in the image. The segmentation results obtained from both methods are similar as shown in Fig 8.a and Fig 8.b. It is evident that the colour change is significant within a few pixels. In Fig 9.b, the boundary appears larger than the boundary obtained from the Live Wire method (shown in Fig 9.a). The presence of a colour gradient along side the original boundary leads to the inclusion of few pixels around the lesion. Fig 10.b shows the detection of the regions within the lesion due to the difference in colour. In Fig 11.b, a small region at the left top corner is incorrectly segmented due to the colour difference. Similarly, in Fig 12.b additional regions were created where the transition from the lesion to the surrounding skin is very smooth. The skin cancer image in Fig 13.a and Fig 13.b, (same as fig. 5) shows accurate segmentation results by both the methods. The disturbances that could be anticipated due to the presence of hairs were overcome by using the adaptive smoothing procedure to obtain the best result. On the other hand, the non use of preprocessing resulted in the identification of the hairs in the skin. In Fig 14.a and 14.b similar segmentation results were obtained. The detection of lesion boundaries by Live Wire method is complex in image such as Fig 15.a but Fig 15.b illustrates an acceptable result by colour texture segmentation. Fig 16.b shows segmentation with extended boundaries. Fig 17.a and Fig 17.b demonstrates the segmentation using Live Wire and colour texture respectively. In this image, the proposed method was able to identify the lesion boundary though there is a variation in colour. Fig 18.a and 18.b shows a good segmentation, but the disturbances such as bubbles in the skin were overcome by using the pre-processing. The result shows that the addition of colour plays a significant part and the inclusion of colour improves the segmentation results [16]. For some results of the segmentation the expertise role of dermatologist is very important.

**Fig 7-18. (a) Segmentation using Live Wire (b) Segmentation using colour texture distributions**

Based on the authors' visual assessment, the boundaries obtained using colour texture segmentation is comparable with the boundaries obtained using Live Wire segmentation. The overall impression was that the two techniques used to identify skin lesions gave results with acceptable boundaries. It is interesting to note that for some images the Live Wire segmentation is different from that of the colour texture segmentation due to colour variation. This raises the question as to where the actual boundaries are, and it appears that different experts use different rules to segment an image. A complete validation can only be performed from expert results by a dermatologist. A more objective impression of the performances of the segmentation and boundary detection schemes can be obtained using a statistical comparison with boundaries drawn by hand by expert dermatologist. The experimental results obtained proved to be encouraging and indicate that the proposed method for colour texture segmentation is appropriate to be applied for detection of skin cancer. The efficient performance of the proposed colour texture segmentation method recognized the boundaries in the skin lesions exactly.

## VI. Conclusion

This work presents a method for the colour texture image segmentation. The proposed method is applied to skin cancer images to identify and demarcate lesion boundaries for expert opinion. The segmentation method is based on the colour and the texture present in the skin cancer images. The distribution of colour features and the distribution of the texture features were used for colour texture discrimination. The distribution of the derived features encompasses both the structural pattern and the colour of the image. This isolates the accurate boundaries of the skin lesions.

## REFERENCES


[1]. http://health.med.umich.edu/healthcontent.cfm?xyzpdqabc=0&id=6&action=detail&AEProductID=HW_Knowledgebase&AEArticleID=hw206547, accessed on 15th October 2008

[2]. Xu, L., Jackowski, M., Ghoshtasby, A., Roseman, D., Bines, S., Yu, C., Dhawan, A., and Huntle, A., 1999, *Segmentation of skin cancer images*. Image and Vision Computing, 65-74.

[3]. Skin Cancer Images. //tray.dermatology.uiowa.edu/DermDB.htm. \http://dermatlas.med.jhmi.edu/derm/IndexDisplay.cfm?ImageID=1061 \http://matrix.ucdavis.edu/tumors/tradition/gallery-melanoma.html, accessed on 15th October 2008.

[4]. Skin Cancer Images. www.cmis.csiro.au/iap/RecentProjects/melanoma, accessed on 15th October 2008.

[5]. Ganster, H., Gelautz, M., Pinz, A.,Binder, M., Pehamberger, H., Bammer, M., and Krocza, J., 1995, *Initial results of automated melanoma recognition.* Theory and Applications of Image Analysis II, Selected papers of the 9th SCIA, Scandinavian Conference on Image Analysis, Uppsala, Sweden.

[6]. Padmapriya, N., Ghita, O., Whelan, P.F., 2004, *Intergration of feature distributions for colour texture segmentation and its applications*, IMVIP, Dublin.

[7]. Grana, C., Pellacani, G., Cucchiara, R., and Seidenari, S., 2003, *A new algorithm for border description of polarized light surface microscopic images of pigmented skin lesions*. IEEE Trans on Medical Imaging, Vol.22, no.8, 959-964.

[8]. Ojala, T., and Pietikainen, M., 1999, Unsupervised texture segmentation using feature distributions. Pattern Recognition, 32:477–486.

[9]. Ojala, T., Pietikainen, M., Harwood, D., 1996, *A comparative study of texture measures based on feature distributions*, Pattern Recognition, Vo1.29, no.1, 51–59.

[10]. Jain, A.K., and Dubes, R.C., 1988, *Algorithms for clustering data.* Prentice Hall, Advanced Reference Series, New Jersey.

[11]. Puzicha, J., Buhmann, J.M., Rubner, Y., and Tomasi, C., 1999, *Empirical evaluation of dissimilarity measures for colour and texture.* In Proceedings of IEEE Int. Conf. on Computer Vision, pp. 1156–1173.

[12]. Ke Chen, 2000, *A feature preserving adaptive smoothing method for early vision.* The Journal of Pattern Recognition Society, Vol.33.

[13]. Padmapriya, N., Ghita, O., Whelan, P.F., 2004, *Integration of feature distributions for colour texture segmentation,* in: Proceedings of the 17th International Conference on Pattern Recognition, Cambridge, UK, pp. 716–719.

[14]. Alexandre, Falcao, X., Udupa, J.K., Samarasekara, S., Sharma, S., Hirsch, B.E., and Lotufo, R.A., 1998, *User-Steered Image Segmentation Paradigms: Live Wire and Live Lane.* Graphical models and image processing, 60:233-260.

[15]. Urschler, M., Mayer, H., Bolter, R., and Leberl, F., 2002, *The LiveWire Approach for the Segmentation of Left Ventricle Electron-Beam CT Images.* In Proccedings of 26th Workshop of the Austrian Association for Pattern Recognition: Vision with Non-traditional Sensors, Publ. Series Österreichische Computer Gesellschaft Vol. 160, pp. 319-326.

[16]. Padmapriya, N., Ghita, O., Whelan, P.F, 2010, *A Generic Framework for Colour Texture Segmentation,* Sensor Review, Vol.30, Issue.1.

## Figures

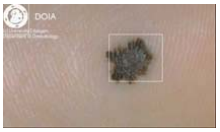

1 (a)

1 (b)

2 (a)

2 (b)

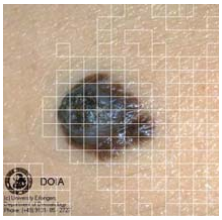

3 (a)

3 (b)

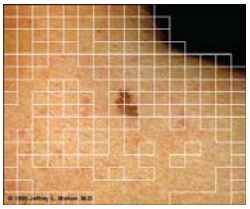

4 (a)

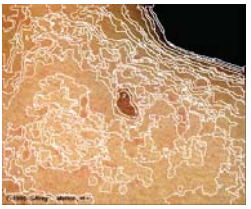

4 (b)

**Fig 1-4 (a) Results after agglomerative merging stage (b) Results after boundary refinement stage**

5 (a)

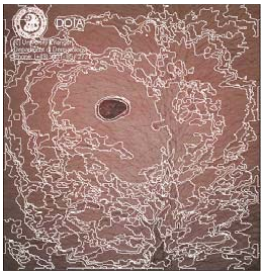

5 (b)

5 (c)

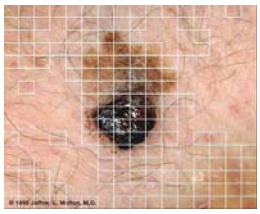

6 (a)

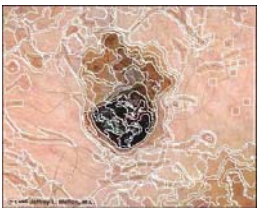

6 (b)

6 (c)

**Fig 5-6. (a) Result after agglomerative merging stage (b) Result after boundary refinement without preprocessing and (c) Result after boundary refinement with preprocessing**

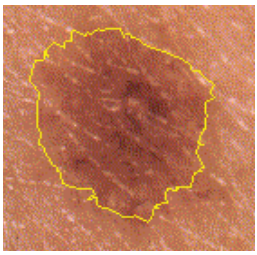

7 (a)

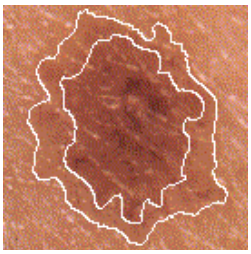

7 (b)

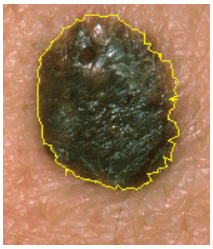

8 (a)

8 (b)

9 (a)

9 (b)

10 (a)

10 (b)

11 (a)

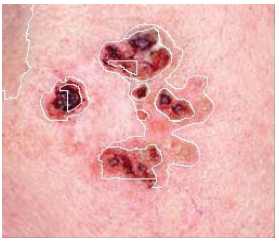

11 (b)

12 (a)

12 (b)

13 (a)

13 (b)

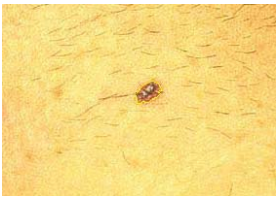

14 (a)

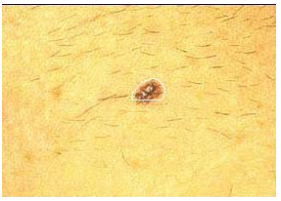

14 (b)

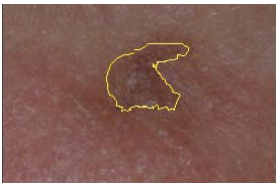

15 (a)

15 (b)

16 (a)

16 (b)

17(a)

17 (b)

18 (a)

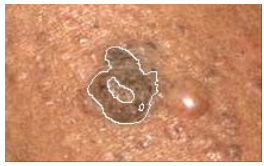

18 (b)

**Fig 7-18. (a) Segmentation using Live Wire (b) Segmentation using colour texture distributions**